Micrometer- and Nanometer-Sized, Single-Crystalline Ribbons of a Cyclic Triphenylamine Dimer and Their Application in Organic Transistors

By *Rongjin Li, Hongxiang Li, Yabin Song, Qingxin Tang, Yaling Liu, Wei Xu,* Wenping Hu,** and *Daoben Zhu**

Triarylamine derivatives are widely used as hole-transport materials in various fields such as in organic electroluminescent (EL) devices.[1–3] Normally, in EL devices molecular materials are required in an amorphous state, so that the injected electrons and holes can be confined in the amorphous layer for efficient EL emission.[3,4] However, molecular materials with high crystallinity are required for organic field-effect transistors (OFETs), so that the semiconductor layer contains as few defects (e.g., disorders, grain boundaries) as possible, that is, the mobility of the molecular materials is as high as possible.[5] The different requirements limit the application of triarylamine derivatives in OFETs.

Shirota (a pioneer of amorphous molecular glasses and organic electroluminescence) suggested that a nonplanar molecular structure could prevent the easy packing of molecules and hence the ready crystallization.[4,6,7] Based on this principle, a series of starburst molecules of triarylamine derivatives was synthesized as amorphous molecular materials.[4,6,7] Contrarily, if the rotation of the phenyl groups of triarylamine derivatives could be restricted and the planarity of the molecules could be improved, the crystallinity of the compounds should be improved. Recently, Song et al. synthesized a new triarylamine derivative as a semiconductor for an OFET with a macrocyclic structure (Fig. 1a, compound **1**).[8] A closed ring and steric crowded structure were used to restrict the rotation of the phenyl groups to increase the molecular planarity, which was different from the linear, star-shaped, or dendrimeric triarylamines. Thin-film OFETs of compound **1** suggested that the mobility of the macrocyclic structure was much higher than that of the linear compound triphenyldiamine.[9–13] In this paper, we will focus on i) the crystallinity of the macrocyclic structure, ii) the synthesis of its micrometer/nanometer-sized single crystals, iii) the transport properties of the micro/nanometer-sized single crystals in OFETs, and iv) the mobility dependence of the micro/nanocrystals on their size. It is expected that the understanding of the structure and property relationship of the macrocyclic structure will be beneficial for the further design and synthesis of materials with high crystallinity and mobility, to further extend their application in OFETs.

Vacuum-deposited thin films of compound **1** showed a series of sharply resolved peaks assignable to multiple (00*l*) reflections in their X-ray diffraction (XRD) patterns,[8] indicating the good crystallinity of this compound in thin films. Transmission electron microscopy (TEM) images of the vacuum-deposited films on a copper grid are shown in Figure 1b and c, and the corresponding selected-area electron diffraction (SAED) pattern is shown in Figure 1d. The SAED pattern of the film confirmed the excellent crystallinity of the macrocyclic structure, which was the basis of controlling the synthesis of single-crystalline structures of the triarylamine derivative.

Physical vapor transport is a well-known technique to grow high-quality single crystals of organic semiconductors.[14] Here, it was extended to compound **1** by using a two-zone horizontal tube furnace.[14] A quartz boat loaded with powders of **1** was placed at the

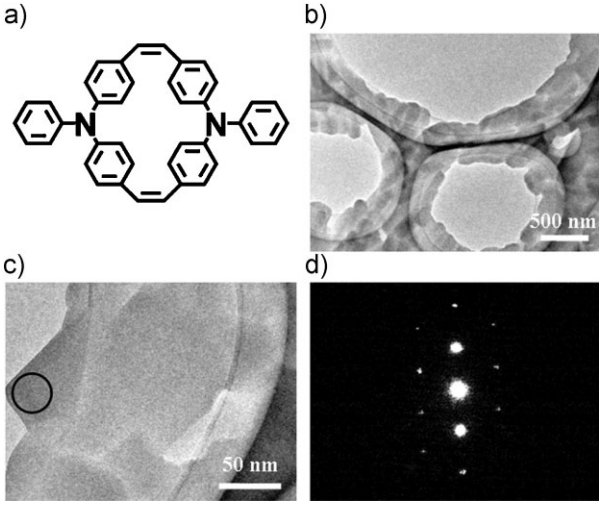

Figure 1. a) Chemical structure of compound **1**. b) TEM image of the deposited film over a large area on a copper grid. c) TEM image of an enlarged area, and d) the corresponding SAED pattern of the selected area (the circled area in c).

[*] Dr. W. Xu, Prof. W. Hu, Prof. D. Zhu, R. Li, Dr. H. Li, Y. Song
Dr. Q. Tang, Y. Liu
Beijing National Laboratory for Molecular Sciences
Key Laboratory of Organic Solids
Institute of Chemistry, Chinese Academy of Sciences
Beijing 100190 (P.R. China)
E-mail: wxu@iccas.ac.cn; huwp@iccas.ac.cn
R. Li, Y. Song, Y. Liu
Graduate School of Chinese Academy of Sciences
Beijing 100039 (P.R. China)

DOI: 10.1002/adma.200802589

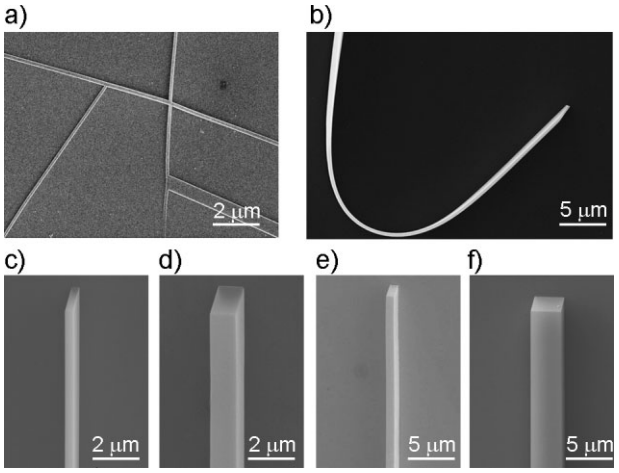

Figure 2. a) Nanometer- and micrometer-sized ribbons of compound **1** produced by the physical vapor transport technique. b) An individual bent ribbon of several tens of micrometers in length. Ribbons with different diameters: c) ~250 nm, d) ~500 nm, e) 1 μm, and f) 4 μm.

high-temperature zone. High purity Ar was used as the carrier gas, and the system was evacuated by a mechanical pump. Products were obtained at the low-temperature zone and characterized by scanning electron microscopy (SEM), X-ray diffraction (XRD), and TEM. As shown in Figure 2, the crystals appeared as micrometer or nanometer-sized ribbons with a regular morphology and a smooth surface. The width of the ribbons ranged from several tens of nanometers to several tens of micrometers, and the length varied from ~15 to 70 μm. Several key factors were found to affect the size and quality of the ribbons, such as the temperature of the zones for material sublimation (T_{sblm}) and crystal growth (T_{growth}). The size of the ribbons could be tuned by the temperature drop between T_{sblm} and T_{growth} ($\Delta T = T_{sblm} - T_{growth}$): the steeper the temperature drop, the thinner the crystals obtained. When T_{growth} was held at 190 °C, the diameter of the crystals could be tuned from several tens of micrometers to several tens of nanometers by changing ΔT from ~50 to ~80 °C. This facile method was useful for the controlled synthesis of ribbons of the triarylamine derivative with different sizes.

The powder X-ray diffraction patterns of the ribbons (see Fig. 3a) showed an intense peak at $2\theta = 6.72°$, which corresponds to a *d*-spacing of 13.14 Å and indicates that the structure of the micrometer and nanometer crystals is the same as that of the bulk crystals of the macrocyclic structure.[8] A typical TEM image of an individual ribbon is given in Figure 3b, and the corresponding SAED pattern is shown in Figure 3c. Several SAED patterns have been indexed with lattice constants obtained from the bulk single-crystal data:[8] $a = 10.642(2)$ Å, $b = 10.657(2)$ Å, $c = 13.974(3)$ Å, $\alpha = 103.89(0)°$, $\beta = 105.11(0)°$, $\gamma = 90.89(0)°$. It can be concluded that the single-crystals grew along the [010] direction, which coincided with the π–π stacking direction of the molecules (Fig. 3d). The diffraction pattern did not change as the electron beam was moved along the crystal, indicating that the whole ribbon was a single crystal. As we know, single crystals not only have prominent merits in the study of intrinsic charge-transport properties of organic semiconductors, but also open up prospects for the fabrication of high-quality devices and circuits.[15,16]

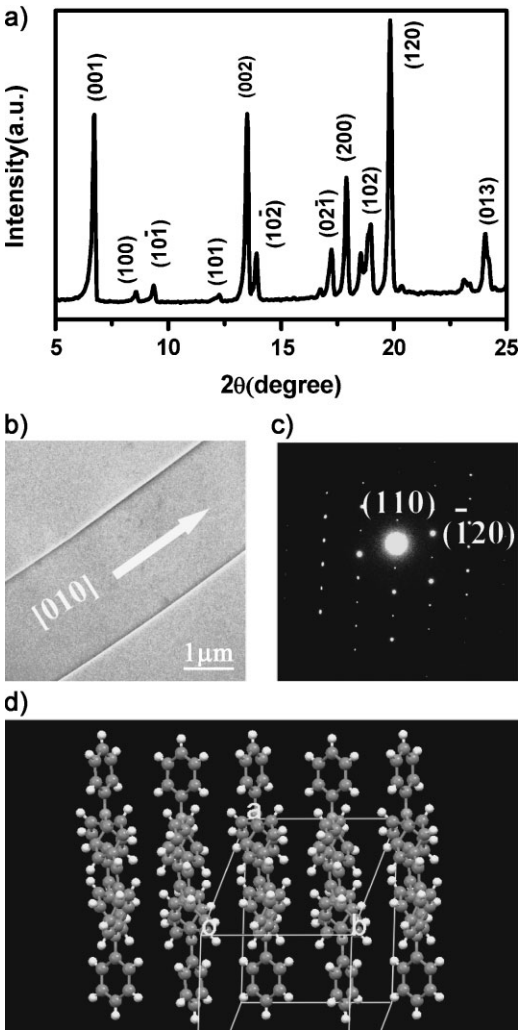

Figure 3. a) Powder diffraction pattern of the ribbons. The peaks were indexed with lattice constants of the bulk crystal. b) TEM images of an individual ribbon and c) the corresponding SAED pattern, indicating that the ribbons grow along the [010] direction. d) Molecular arrangement in the ribbon.

For the potential application of the ribbons in devices, for example, in OFETs, it is important to grow them in situ directly onto a substrate, so that the disadvantages of the handpicking process of crystals from one place to another (e.g., a substrate) for the fabrication of devices could be avoided. Previously, we demonstrated that nanoribbons of CuPc and F_{16}CuPc could be grown in situ on a SiO_2 surface.[17,18] Fortunately, the micrometer and nanometer ribbons of compound **1** could be patterned in situ on octadecyltrichlorosilane (OTS)-modified SiO_2 substrates by the same technique. The exemplified patterned ribbons with different sizes are shown in Figure 4. These patterned ribbons are not only free from surface pollution and damage of single crystals, but also provide a high-quality crystal/SiO_2 interface for devices.

As an example of the application of the single-crystalline ribbons, OFETs of individual ribbons were fabricated (as shown in Fig. 5a) by the 'multitime gold-wire mask moving' technique[19] based on the in situ patterned ribbons of compound **1**. Over

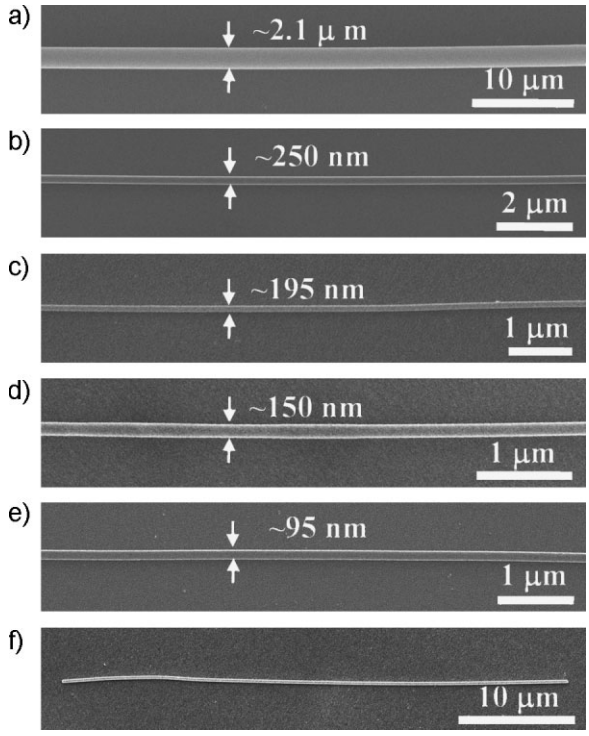

Figure 4. In situ patterned ribbons of compound **1** with different size on OTS-modified SiO_2: a) 2.1 μm, b) 250 nm, c) 195 nm, d) 150 nm, e) 95 nm, and f) an individual ribbon several tens of micrometers long.

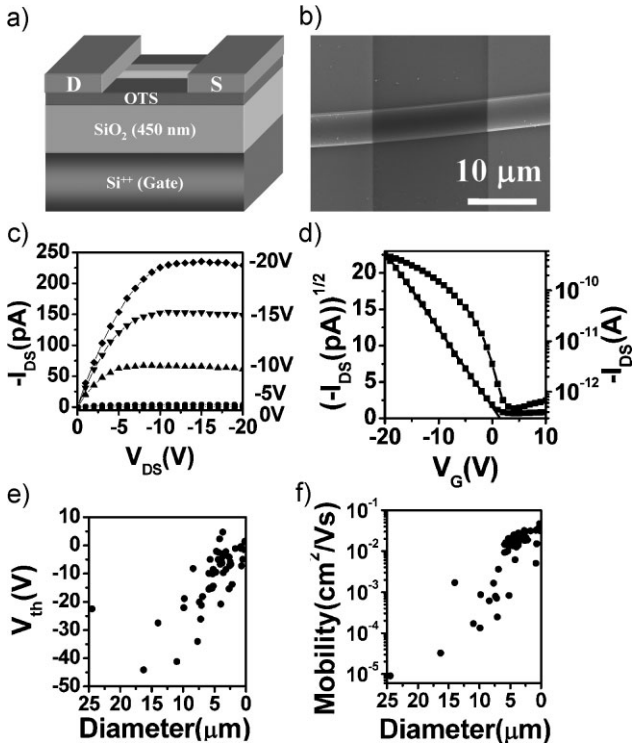

Figure 5. a) Schematic diagram and b) SEM images of the devices with an individual ribbon, c) output and d) transfer characteristics (channel length, $L = 17.9$ μm, channel width, $W = 190$ nm) of the devices, and e) mobility and f) threshold voltage distribution of 50 devices as a function of crystal size.

50 devices of individual ribbons with different sizes have been constructed. The width of the ribbons used ranged from several tens of nanometers to several tens of micrometers (see Supporting Information, Fig. S1). An exemplified device is shown in Figure 5b, and typical output and transfer characteristics are shown in Figure 5c and d. The output characteristics (Fig. 5c) show highly linear and saturation characteristics without obvious contact resistance. Figure 5d shows the transfer characteristics of the device. The field-effect mobility of the device was estimated at around 0.032 $cm^2\ V^{-1}\ s^{-1}$ from the saturation region, and the on/off ratio of the device was calculated at $\geq 10^3$ with a threshold voltage of 1.4 V. To the best of our knowledge, the mobility is one of the highest of the triarylamine derivatives.

It was found that the mobility of the single-crystalline devices was dependent on the size of the crystals used. When crystals with a width greater than 6 μm were used, the devices exhibited mobility lower than 0.001 $cm^2\ V^{-1}\ s^{-1}$, and the mobility of the devices increased rapidly from below 0.001 to ~0.05 $cm^2\ V^{-1}\ s^{-1}$ when the width of the single crystals decreased from ~6 μm to ~200 nm. The mobilities of the 50 devices with different ribbon widths are shown in Figure 5f. This 'size effect' is tentatively explained by three factors. First, the smaller the crystal, the higher the quality. It is well known that nanometer-sized crystals are typically defect free.[20] As the crystals grow larger, more lattice defects (point, linear, and planar) may appear and deteriorate the device performance. For example, dislocations in real crystals are typically in the order of $10^{6-8}\ cm^{-2}$, and most are introduced in the crystals during growth.[21] Similar results were found by Bao and coworkers for rubrene single crystals, which confirmed that the thinner crystals were nearly defect-free on the surface, while the thicker crystals showed more frequent and much larger surface steps.[22] The lowering of the threshold voltage with a decrease in crystal size (Fig. 5e) also supports this assumption, because the threshold voltage is proportional to the concentration of charge-carrier traps.[23] Second, the smaller/thinner crystals are more flexible, and have a better physical contact to the substrate. As described previously, the in situ patterning of the single-crystalline ribbons depends on the softness of the nanoribbons and the weight of the ribbon itself.[17,18] The large size of the microribbons results in a strong rigidity, such that the weight of the ribbon itself is not enough to bend it down onto the substrate. This will also lead to a decrease in the device performance with an increase in crystal size. The third possibility is that devices based on big/thick crystals (several micrometers to several tens of micrometers in diameter) have a relatively large contact resistance, because in top-contact devices carriers need to cross the thickness of the crystal twice from the source to the drain. If the crystal is thick, the contact resistance may be large at a low drain–source voltage (V_{DS}), so that the drain–source current is decreased. It was found that the output curve was more or less nonlinear at low V_{DS} for devices based on large crystals (typical in devices with a crystal diameter >1 μm), which indicates the existence of contact resistance, while for devices based on small crystals (diameter <1 μm), the output characteristics showed highly linear characteristics at a low V_{DS} without obvious contact

resistance (see Fig. 5c). These merits indicate that small crystals are more convenient to circumvent the contact resistance for the fabrication of high-performance transistors, at least for devices with top-contact configurations.

It is important to note that the obtained mobility mentioned in this study means the effective mobility, which depends on device physics. This is very common in organic transistors, such as the transistors of rubrene. Podzorov and coworkers demonstrated that the mobility of single-crystal rubrene was 0.1–1 $cm^2 V^{-1} s^{-1}$ at room temperature with a thin parylene films as the gate insulator.[24] However, the elastomeric transistor stamp technique could enable the mobility of rubrene to increase to 15 $cm^2 V^{-1} s^{-1}$.[25] And the 'air-gap' transistor stamp technique refreshed the mobility up to ~20 $cm^2 V^{-1} s^{-1}$ at 300 K.[23] The mobility dependence on the interface/insulator was also confirmed by other scientists such as Stassen et al.,[26] who found the mobility of rubrene could change from 10 to 15 $cm^2 V^{-1} s^{-1}$ upon increasing the relative dielectric constant,[26] and suggested the mobility of organic single-crystal transistors depended not only on the specific molecule used, but was also an intrinsic property of the crystal/dielectric interface.[26] Jurchescu et al. suggested that high-mobility organic transistors were interface controlled.[27] All the results indicate the importance of the device physics, for example, Palstra and coworkers were able to measure the intrinsic properties of a single crystal by careful control of the interface properties, to minimize the trap density in the active channel.[27] The selection of 'small' crystals instead of 'large' crystals is probably an effective way to approach this point.

In summary, high-quality single-crystalline ribbons of compound **1** have been successfully synthesized with sizes tuned from micrometers down to nanometers. The ribbons could be patterned in situ on a SiO_2 substrate for device applications. A series of organic transistors were fabricated based on individual ribbons with field-effect mobilities up to 0.05 $cm^2 V^{-1} s^{-1}$. To the best of our knowledge, the mobility is one of the highest results of the triarylamine derivatives. Moreover, the mobility of the devices depended greatly on the size of the ribbons; the smaller the crystal, the higher the mobility of the transistors observed, which indicates that 'small' crystals, that is, nanocrystals, are more appropriate for the fabrication of high-performance devices.

Experimental

The SiO_2/Si substrates used in this study were successively cleaned using deionized water, acetone, and ethanol. The cleaned substrates were modified with OTS by a vapor deposition method. Thin-film samples for TEM observation were deposited on a Cu grid covered with an amorphous carbon film. The deposition rate was controlled below 0.1 Å s^{-1}. Single crystals of compound **1** were grown by a physical vapor transport (PVT) method in a horizontal tube furnace. SEM images were obtained using a Hitachi S-4300 (Japan). TEM and SAED were carried out using a JEOL 2010 (Japan). X-ray diffraction (XRD) was measured on a D/max2500 with a Cu Kα source ($k = 1.541$ Å). FET characteristics were measured using a Keithley 4200 SCS and a Micromanipulator 6150 probe station in a clean and shielded box at room temperature in air.

Acknowledgements

The authors acknowledge the financial support from National Natural Science Foundation of China (20721061, 20872146, 60736004, 50725311, 60771031), Ministry of Science and Technology of China (2006CB806200, 2006CB932100), and Chinese Academy of Science. Supporting Information is available online from Wiley InterScience or from the author.

Received: September 2, 2008
Revised: October 10, 2008
Published online: January 29, 2009

[1] J. Kido, Y. Okamoto, *Chem. Rev.* **2002**, *102*, 2357.
[2] U. Mitschke, P. Bäuerle, *J. Mater. Chem.* **2000**, *10*, 1471.
[3] R. H. Friend, R. W. Gymer, A. B. Holmes, J. H. Burroughes, R. N. Marks, C. Taliani, D. D. C. Bradley, D. A. D. Santos, J. L. Brédas, M. Lögdlund, W. R. Salaneck, *Nature* **1999**, *397*, 121.
[4] Y. Shirota, *J. Mater. Chem.* **2005**, *15*, 75.
[5] C. Reese, Z. Bao, *Mater. Today* **2007**, *10*, 20.
[6] Y. Shirota, *J. Mater. Chem.* **2000**, *10*, 1.
[7] Y. Shirota, H. Kageyama, *Chem. Rev.* **2007**, *107*, 953.
[8] Y. Song, C. Di, X. Yang, S. Li, W. Xu, Y. Liu, L. Yang, Z. Shuai, D. Zhang, D. Zhu, *J. Am. Chem. Soc.* **2006**, *128*, 15 940.
[9] C. H. Cheung, K. C. Kwok, S. C. Tse, S. K. So, *J. Appl. Phys.* **2008**, *103*, 093 705.
[10] T. P. I. Saragi, T. Fuhrmann-Lieker, J. Salbeck, *Adv. Funct. Mater.* **2006**, *16*, 966.
[11] A. Cravino, S. Roquet, O. Alévêque, P. Leriche, P. Frère, J. Roncali, *Chem. Mater.* **2006**, *18*, 2584.
[12] T. P. I. Saragi, T. Fuhrmann-Lieker, J. Salbeck, *Synth. Met.* **2005**, *148*, 267.
[13] M. Sonntag, K. Kreger, D. Hanft, P. Strohriegl, S. Setayesh, D. de Leeuw, *Chem. Mater.* **2005**, *17*, 3031.
[14] C. Kloc, P. G. Simpkins, T. Siegrist, R. A. Laudize, *J. Cryst. Growth* **1997**, *182*, 416.
[15] R. W. I. de Boer, M. E. Gershenson, A. F. Morpurgo, V. Podzorov, *Phys. Status Solidi A* **2004**, *201*, 1302.
[16] C. Reese, Z. Bao, *J. Mater. Chem.* **2006**, *16*, 329.
[17] Q. Tang, H. Li, Y. Song, W. Xu, W. Hu, L. Jiang, Y. Liu, X. Wang, D. Zhu, *Adv. Mater.* **2006**, *18*, 3010.
[18] Q. Tang, H. Li, Y. Liu, W. Hu, *J. Am. Chem. Soc.* **2006**, *128*, 14 634.
[19] Q. Tang, H. Li, M. He, W. Hu, C. Liu, K. Chen, C. Wang, Y. Liu, D. Zhu, *Adv. Mater.* **2006**, *18*, 65.
[20] R. L. Penn, J. F. Banfield, *Science* **1998**, *281*, 969.
[21] I. Sumagawa, in *Crystals Growth, Morphology, and Perfection*, Cambridge University Press, New York, US **2005**, Ch. 6.
[22] A. L. Briseno, R. J. Tseng, M. M. Ling, E. H. L. Talcao, Y. Yang, F. Wudl, Z. Bao, *Adv. Mater.* **2006**, *18*, 2320.
[23] V. Podzorov, E. Menard, A. Borissov, V. Kiryukhin, J. A. Rogers, M. E. Gershenson, *Phys. Rev. Lett.* **2004**, *93*, 086 602.
[24] V. Podzorov, V. M. Pudalov, M. E. Gershenson, *Appl. Phys. Lett.* **2003**, *82*, 1739.
[25] V. C. Sundar, J. Zaumseil, V. Podzorov, E. Menard, R. L. Willett, T. Someya, M. E. Gershenson, J. A. Rogers, *Science* **2004**, *303*, 1644.
[26] A. F. Stassen, R. W. I. de Boer, N. N. Iosad, A. F. Morpurgo, *Appl. Phys. Lett.* **2004**, *85*, 3899.
[27] O. D. Jurchescu, M. Popinciuc, B. J. van Wees, T. T. M. Palstra, *Adv. Mater.* **2007**, *19*, 688.